

# **SIMULTANEOUS DAMAGE DETECTION AND DEFLECTION MEASUREMENT OF MORPHING WING STRUCTURES BY FIBER OPTIC SENSING SYSTEM**

**Zoran Djinovic<sup>1</sup>, Michael Scheerer<sup>2</sup>, Milos Tomic<sup>3</sup>, Marijana Stojkovic<sup>1</sup>, Martin Schueller<sup>4</sup>**

<sup>1</sup> *Austrian Center for Medical Innovation and Technology GmbH, 2700 Wiener Neustadt, Austria*

<sup>2</sup> *Aerospace & Advanced Composites GmbH, 2700 Wiener Neustadt, Austria*

<sup>3</sup> *School of Electrical Engineering, University of Belgrade, 11120 Belgrade, Serbia*

<sup>4</sup> *Fraunhofer Institute for Electronic Nano Systems, 09126 Chemnitz, Germany*

zoran.djinovic@acmit.at

## **ABSTRACT**

In this paper we present results of investigation of simultaneous damage detection and deflection measurement of morphing CFRP honeycomb structure by fiber optic sensing system developed in the frame of EU-FP7 project “Fiber Optic System for Deflection and Damage Detection (FOS3D)”. The system is based on low- and high-coherence interferometry performed as “all-in-fiber” sensing configuration. Raw signals have been on- and off-line processed by “arctang” algorithm. Deflection data, expressed as phase angle change of the interferometer, have been simultaneously acquired with the reference data. A linear relationship between the fiber-optic sensing and reference technique is obtained. Slope of the linear fit line of 8 rad/mm denotes sensitivity of this sensor. Noise floor of about  $\pm 70 \mu\text{rad}/\sqrt{\text{Hz}}$  determines the lowest measurable wing deflection of about 6  $\mu\text{m}$ . Damage events have been simulated by pencil break and hammer impact with- and without damages over the CFRP honeycomb structure. Raw fiber-optic interference and reference acoustic emission sensor signals have been simultaneously acquired. Figure of merit is given as probability of detection (POD) and localization of simulated impact event. All events can be detected and located with a POD of more than 98% within the localization error of around 15 mm.

**KEYWORDS:** *structural health monitoring, fiber-optic sensors*

## **INTRODUCTION**

The morphing wing concept of aircrafts finds a deep inspiration in the flight capabilities of birds [1]. It has to assure different flight manoeuvres in a wide range of environmental conditions just as current aircrafts. Every operational task has to be accomplished efficiently, safety and reliable [2]. For this purpose it is necessary to have complex mechanical structures and materials capable to actively change the aerodynamic shape of the wing [3]. Carbon- or glass-fiber reinforced plastics (CFRP, GFRP) have already found application in modern aircrafts and in morphing field as well. Honeycomb structures equipped with different actuators are suitable for the morphing purpose [4]. In a real application it is necessary to have a closed loop between the actuators and sensors, which are responsible for providing feedback information about the real time position of the wings. During morphing action materials and structures suffer large loadings, which eventually could lead to the damage. Therefore, sensors have to assure on board structural health monitoring (SHM) of the structure in order to avoid any catastrophic scenarios.

In this paper we present results of investigation of simultaneous damage detection and deflection measurement of morphing CFRP structure by fiber optic sensing system developed in the frame of an EU-FP7 project named “Fiber Optic System for Deflection and Damage Detection (FOS3D)” [5]. The system is based on low- and high-coherence interferometry performed as “all-in-fiber” sensing configuration. It is composed of four fiber-optic sensors, which are adhesively bonded onto the CFRP honeycomb structure. Interference signals were obtained by recombination of back reflected signals from the fiber tips of sensing and reference arms. Raw signals have been on- and off-line processed by “arctang” algorithm. Output result is voltage phase angle signal of every particular interferometer, which depends on the deflection magnitude. Deflection data have been acquired by reference technique using an inductive displacement sensor. A linear relationship between the fiber-optic sensing and reference techniques was obtained. Slope of the linear fit line of about 8 rad/mm denotes sensitivity of this sensor. Noise floor of about  $\pm 70 \mu\text{rad}/\sqrt{\text{Hz}}$  determines the lowest measurable deflection of about 6  $\mu\text{m}$ .

Damage events have been simulated by pencil break and hammer impact with- and without damages over the CFRP structure. Four raw interference and four reference signals obtained by acoustic emission sensors have been simultaneously acquired by the conventional Acoustic Emission (AE) system. After signal processing of both kinds of AE signals damage detection procedure was accomplished. Figure of merit is given as probability of detection (POD) of simulated impact events. All events can be detected and located by the algorithm of zonal detection with a POD of more than 98% that is equal to the reference system. Nevertheless all damaging impacts can be detected and located with an average localization error of around 15 mm with both systems.

## 1 PRINCIPLE OF OPERATION

Basic principle of simultaneous wing flap deflection measurement and damage detection is an optical phase change occurred in the sensing coil of a fiber optic Michelson interferometer, Figure 1a. Fiber optic 3x3 single-mode (SM) coupler splits light emitted by source LS, a superluminescent diode (SLD) of 50  $\mu\text{m}$  of coherence length at 1300nm, into the three arms. One of the arms (so called inert arm) is terminated by cleaving of the fiber end at 8° in order to suppress back reflection of spurious light beam, which could be a source of intensity noise. The other two arms form the sensing and reference fiber optic coils. Light beam travels toward the fiber tips of both arms and reflects back from the fiber end surfaces and returned to the 3x3 coupler to recombine. Recombined light signals, carrying information of the optical path length difference (OPD) between the sensing and reference arms, hit the two receiving InGaAs photodiodes (PD1, PD2) generating voltage signals.

The sensing and reference coils are firmly fixed to the wing structure and sustain the static deformation originating from the wing deflection. Simultaneously, the coils sense the acoustical waves traveling through the wing structure, caused by an external impact or structure crack damage.

Sensing configuration, depicted in Figure 1a, is basically a classical two beam interferometer where irradiance at photodiodes is given by:

$$I_{PD} = I_1 + I_2 + 2 \cdot \sqrt{I_1} \cdot \sqrt{I_2} \cdot |\gamma_{11}(\Delta L_{12})| \cdot \cos(2 \cdot k \cdot \Delta L_{12}) \quad (1)$$

where  $\Delta L_{12} = L_1 - L_2$ ,  $L_1$  and  $L_2$  are length of sensing and reference coils,  $I_1$  and  $I_2$  are irradiances of beams reflected from the mirrored end of the sensing and reference fibers,  $k = 2\pi/\lambda$  is wave number of light and  $\gamma_{11}$  is the degree of coherence of light.

When an external force acts on the fiber that carries an optical signal, it induces a change of the optical path length in the sensing arm. There are two basic mechanisms to produce the phase change: direct and indirect coupling of strains to the fiber and thermal effects. Hence, the phase change induced by the applied load is given by the expression (2) [6]:

$$d\phi = k \cdot d(n \cdot L) = k \cdot L \cdot \left( n \frac{dL}{L} + dn \right) \quad (2)$$

where:  $n$  is the refractive index of glass in the core region and  $L$  is the overall sensing length of the fiber. The term  $ndL$  reflects the physical change of the fiber length while the term  $Ldn$  reflects the change of the refraction index of the glass.

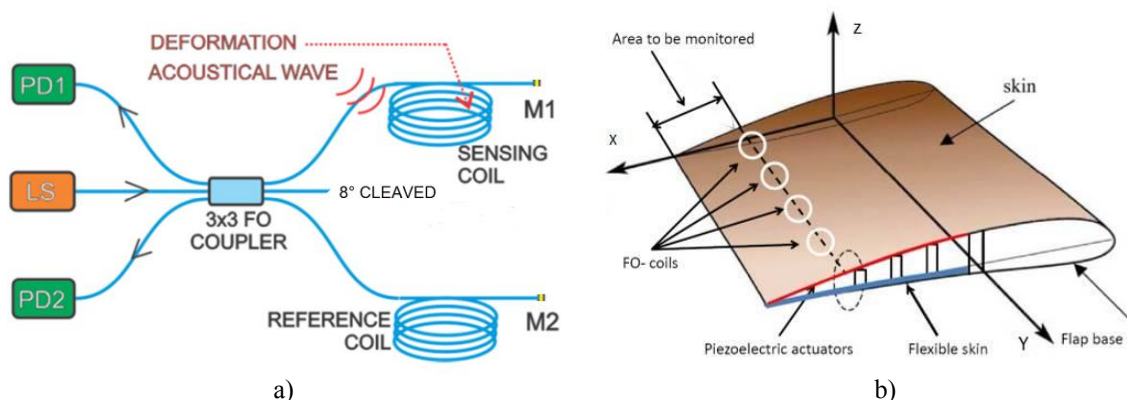


Figure 1: a) Base sensing configuration: Michelson interferometer with 3x3 fiber optic coupler; “deformation”-perturbation caused by wing deflection, “acoustical wave”-produced by damage-like events; M1, M2-mirrors (fiber tips), PD1, PD2-photodiodes, LS-light source; b) Schematically presentation of placement of fiber-optic sensors over the morphing wing structure in the area to be monitored

Figure 1b presents overall configuration of morphing wing structure equipped with an array of circular (or elliptical) shape fiber-optic sensors, which are connected to the 3x3 couplers (Figure 1a) and multiplexed in a common sensing system (see Figure 2)[7]. In the, so called, single sensing configuration, only sensing coil is adhesively bonded over the morphing area, while reference coil is suited in a proximity of the first one. In the push-pull configuration one coil is on the top and other on the bottom side of the wing. Such a configuration is applied in this work because of normalization of parasitic effect, e.g. temperature, typically occurred in the subjected CFRP structure. Maximal required wing deflection is  $\pm 5^\circ$  with resolution of  $0.1^\circ$  and damage of about 20mm in diameter with a location accuracy of 5% in respect to the average sensor spacing.

Combination of low- and high-coherence radiation allows: 1) absolute determination of morphing wing position in respect of the initial (typically non-deformed) wing position (the role of the low-coherence source) and deflection measurement in the entire range of  $\pm 5^\circ$  (the role of the high-coherence source). Damage detection is provided by acquisition, band pass filtration from 5 kHz to 500 kHz and processing of just one high-coherence interference signals. Determination of morphing wing deflection is performed by signal processing using “arctang” algorithm of low-frequency (of about 100Hz) raw interference signals.

## 2 SYSTEM DESIGN

The concept of the system is schematically presented in Figure 2. Here is applied, so called, push-pull sensing configuration because one sensing coil is on the top of the subjected CFRP structure and other is underneath on the bottom side of the CFRP structure at the same coordinate in respect of the overall dimensions of the plate of 400x200x50mm. The plate has a specific triangular shape in longitudinal cross-section.

The entire setup is composed of four multiplexed fiber-optic sensors denoted by S1-S4. Both (sensing and reference) sensors are in the coil form of 20mm in diameter with just one turn, which are adhesively bonded onto CFRP structure. They are made by turning of single-mode optical fiber Corning e28+. Both coils are parts of the output arms of a 3x3 coupler which is used to build up two Michelson interferometers. It is of primary importance to say that both arms, including sensing coils, are short having of about 200mm in length. The length of the arm was precisely adjusted so the every interferometer was set to be in the equilibrium state when sensitivity of sensors was maximal. By this approach a substantial benefit in respect of better stability of interference working

point and eventually higher SNR is obtained. Static phase of the arms are mutually shifted for about  $120^\circ$  that assures obtaining of quasi-quadrature interference signals.

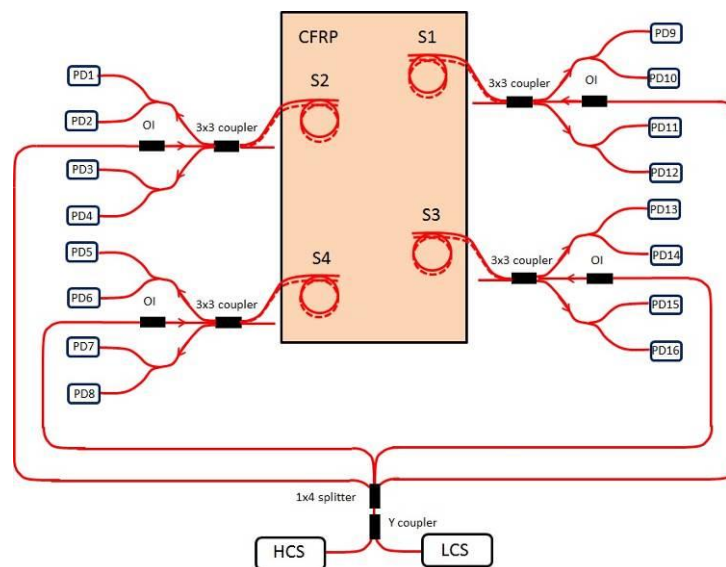


Figure 2: Schematic presentation of multiplexed LCS\_HCS sensing configuration composed of four fiber-optic sensors: S1-S4. Testing structure: CFRP honeycomb plate in size of 400x200x50 mm. HCS high-coherence source, LCS low-coherence source, photodiodes PD1, PD3, PD5, PD7, PD9, PD11, PD13, PD15 (HCS), PD2, PD4, PD6, PD8, PD10, PD12, PD14, PD16 (LCS), OI optical isolator, WDMC wavelength division multiplexing coupler

The interferometers are supplied by high- and low-coherence radiation generated by high- and low-coherence sources emitting at 1550nm and 1310nm of light wavelength, respectively. Both radiations are combined by a “Y shape” wavelength division multiplexing coupler (WDMC) and further distributed, via a 1x4 splitter, towards every single sensor into the middle input arm of the 3x3 coupler. Interference signals were obtained by recombination of back reflected signals from the fiber tips of the sensing and reference output arms. Two interference signals of one sensor are bifurcated by WDM “Y splitter” to four photodiodes. The WDM splitter separates raw interference signals in a way to have a couple of two high- and a couple of two low-coherence signals. Therefore we have 16 photodiodes, which signals simultaneously get into the FOS3D sensing system depicted in Figure 3.

### 3 EXPERIMENT

Figure 3 shows an overall view of the FOS3D sensing system and loading rig together with the subjected CFRP honeycomb structure. The FOS3D sensing system consists of: two-channel DC power supply, high- and low-coherence light sources (HCS, LCS), FOS3D16TIA- 16 InGaAs photodiodes with accompanied transimpedance amplifier and four FOS3D DEF/DAM unit.

Top side of the CFRP structure, depicted in Figure 4a, is equipped with four fiber-optic sensors, four piezo-ceramic transducers (PZT) and four strain gauges. Bottom side of the structure is of the same sensors configuration and two inductive sensors touching the CFRP structure. Four input and eight output arms of the four 3x3 couplers were connected to the FOS3D sensing system. During deflection (from 0 to 10mm) and damage test campaigns, data acquisition of on-line calculated phase signal, raw high-coherence photodiode signals and accompanied reference signals from inductive sensors have been done by 16bit NI DAQ and by a commercial Acoustic Emission system.

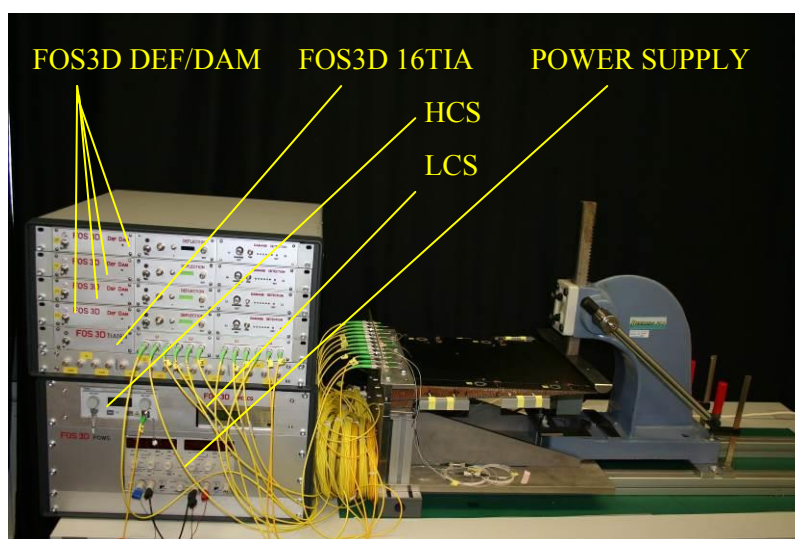


Figure 3: Overall view of the entire FOS3D sensing system and loading rig, LCS low-coherence source, HCS high-coherence source

Figure 4b illustrates the same CFRP structure exposed to the compression loading in a tensile test machine for final test. Here we induced cyclic loading from 0 to 15mm and from 0 to 20mm of deflection. Deflection was directly measured by stroke of the machine. Number of cyclic loading was three, five and ten. During this testing several signals have simultaneously been acquired: eight strain gauges for strain measurement, eight PZT for acoustic signal measurement, and all aforementioned fiber-optic signals.

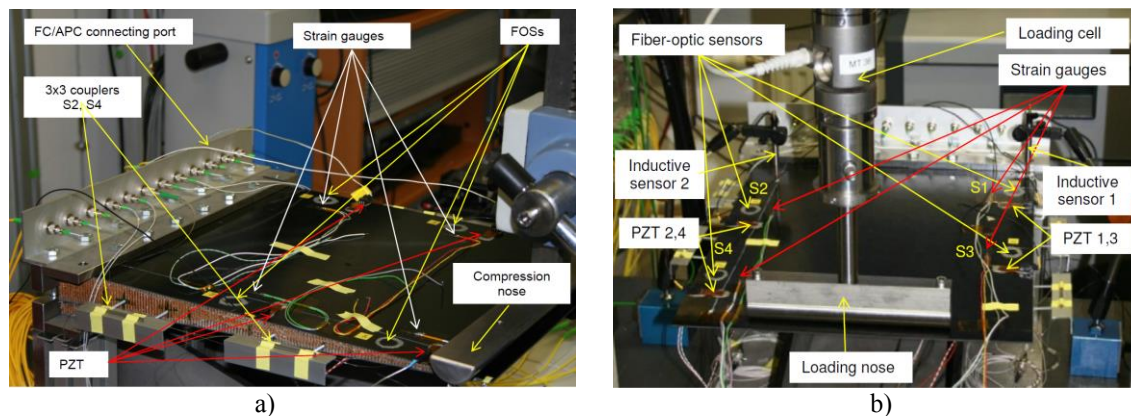


Figure 4: CFRP structure of 400x200x40mm in size equipped with four fiber-optic sensors denoted by yellow marks from S1 to S4, four PZT acoustic emission sensors and four strain gauges in close proximity of FOSs;  
a) testing by laboratory rig and b) testing by compression using a tensile test machine

#### 4 RESULTS AND DISCUSSION

Figure 5a shows a screen shots of raw interference signals, two of high-coherence (red and green) and two of low-coherence (gray and yellow), acquired from the fiber-optic sensor S4 during loading for deflection of 5,5mm. Looking from the left to the right of the diagrams we can see a periodic structure of all four signals that corresponds with interference patterns occurring in the interferometer. From these signals the “arctang” algorithm [8] calculates the phase angle change as output signal shown in Figure 5b. In the two small square-shape graphs, at the right side of the diagrams, we can follow up the Lissajous presentation of the low-(left) and high-(right) coherence signals.

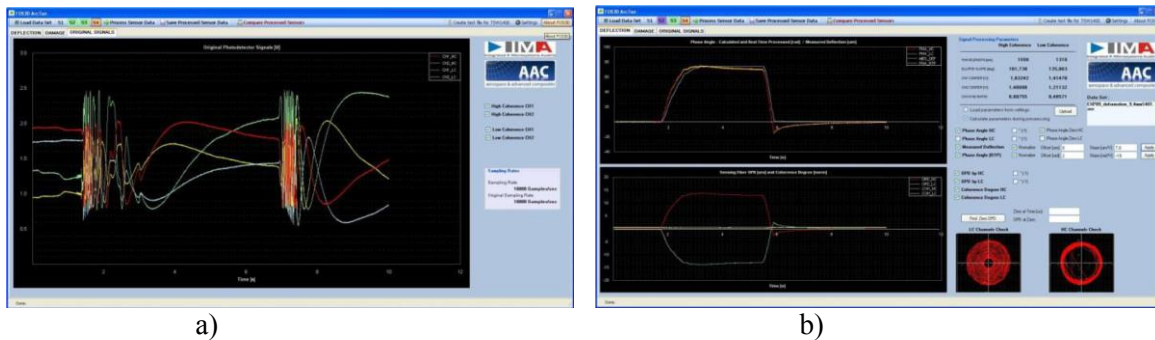


Figure 5: a) Raw interference voltage signals acquired for the case of deflection measurement of 5,5mm; high-coherence signals (red, green), low-coherence signals (grey, yellow), (b) Phase angle signals; on-line (yellow) and off-line (red) calculated, reference signal (grey) (all from upper graph), optical path difference (OPD) (red), coherence degree of low- (yellow) and high-coherence (white) signals (all from lower graph)

Figure 6a presents a linear relationship between the phase angle measured in fiber-optic sensor versus deflection of subjected CFRP structure. Out of this diagram we determined sensitivity of every particular sensor as a slope of the liner fitting line. Sensor sensitivity depends on its position on the CFRP structure. For example, sensor S1 demonstrates the largest sensitivity since at this place the CFRP structure and naturally optical fiber of sensor S1 are exposed to the highest strain. Other two sensors S2 and S3 show gradually smaller sensitivity, while sensor S4 shows the smallest sensitivity as it was found by the final test under the tensile test machine.

Minimal measurable deflection value by the FOS3D system is determined by finding the noise floor of the overall system. Figure 6b presents typical noise signal of fiber-optic sensors recorded by generation of minimal deflection of  $35\mu\text{m}$ . The main noise source is about 10mV, which determines the minimal detectable phase angle signal of about 60 mrad, i.e. minimal detectable deflection of about 6-7 $\mu\text{m}$ . This is much better than required resolution of about 200 $\mu\text{m}$ .

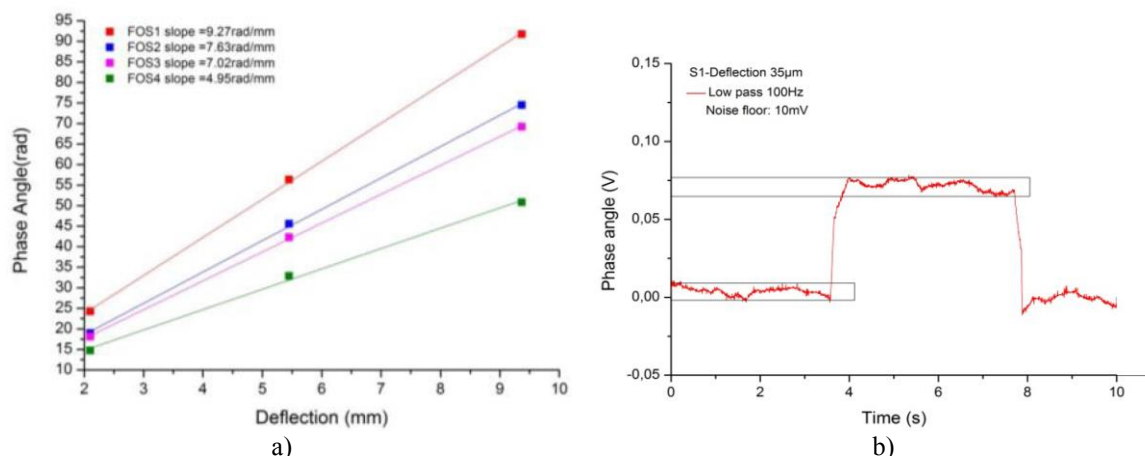


Figure 6: a) Calibration diagram of phase angle vs. deflection of all four sensors  
b) Minimal detectable phase angle (V) of fiber-optic sensor S1 ( $\sim 6\mu\text{m}$  of deflection)

Figure 7 summarizes results of simultaneous deflection measurement and damage detection in case of cyclic loading from zero to 15mm of total deflection. CFRP structure was exposed to the hammer impact at around 240s of deflection experiment (denoted by ellipse) as can be seen out of Figure 7a. The hammer impact produced a sudden phase change that appeared as jump of voltage signal, depicted in the inset. Figure 7a shows voltage signal of fiber-optic sensors in dependence on deflection (stroke) recorded by tensile test machine. Figure 7b shows calibration diagram of phase angle change in radians versus strain which is obtained for the case of simultaneous deflection

measurement and damage detection. Sensitivity of all fiber optic sensors was determined as a slope of linearly fitted line (yellow) and it is of about  $0,1 \text{ rad}/\mu\epsilon$ .

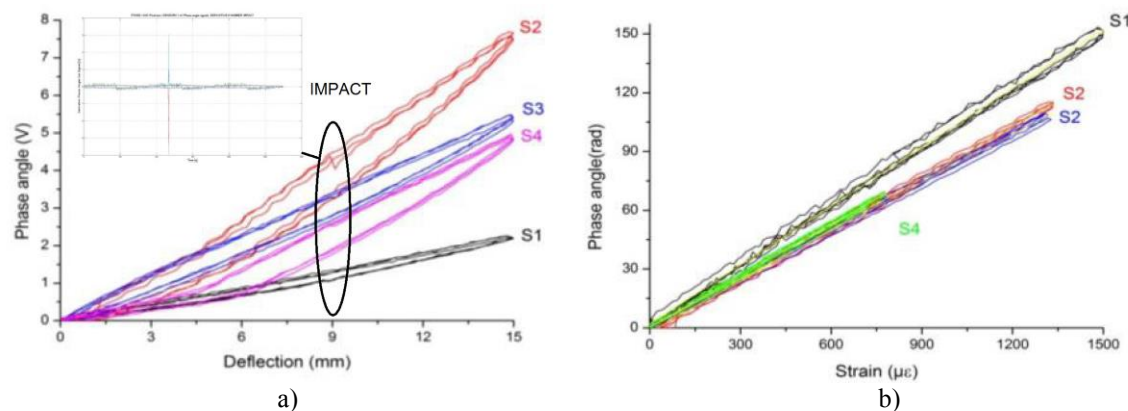


Figure 7: Results of simultaneous deflection measurement and damage detection: a) Phase angle voltage signals of fiber-optic sensors for 15mm. Inset: phase change due to impact b) Calibration diagram of phase angle vs. strain for all four fiber-optic sensors for 15mm of deflection; yellow -linear fit line

Figure 8a presents common results of damage detection produced by different types of impact: pencil breaks (small- non-damaging), non-damaging impacts with an impact hammer; damaging impacts with an impact hammer, damaging impact during morphing of the CFRP structure. All impacts have been analysed regarding detectability and localization using zonal and 2D localization algorithm, where the arrival time of the signals at the individual sensors were determined using first threshold crossing.

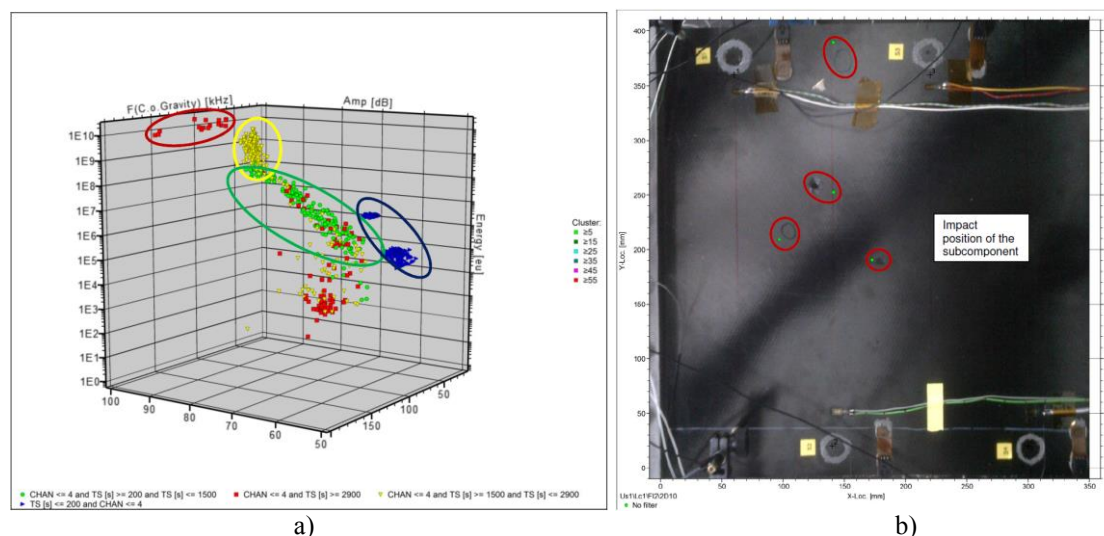


Figure 8: a) Energy as function of the amplitude and average frequency of the detected AE hits (blue dots: calibration /green dots: pencil breaks / yellow dots: non damaging impacts / red dots: damaging impacts) b) Position of the located impacts for all three impacts measured by the FOS3D system. The damaged honeycomb panel is shown in the background to illustrate the real impact positions compared to the located impact position by the FOS3D system

The most sensitive parameter for damage detection is the AE energy and the average frequency. All pencil breaks, non-damaging impacts and damaging impacts produce hits with a large scatter band of parameters. Figure 8a illustrates three different clusters of hits: red cluster: first hits due to damaging impacts, yellow cluster: first hits due to non-damaging but higher energetic impacts, green cluster: hits from pencil breaks and reflections from the boundaries of the non-

damaging and damaging impacts. Only the data from the red cluster serve as the basis for the detection of damaging impacts. They are obtained after data filtering for: amplitude  $> 95$  dB, average frequency  $> 80$  kHz and energy  $> 1 \times 10^9$ . All damaging impacts can be located with a 2-D localization algorithm using the threshold crossing for the determination of the arrival time (preferred localization algorithm) within an average localization error of less than 15 mm, shown in Figure 8b. All events can be detected and located with a POD of more than 98%. Due to the energy of the damaging impacts the quick S0 mode is strong enough to trigger all sensors which is required for the proper function of the mentioned localization algorithm.

## CONCLUSION

Main characteristic of transportable FOS3D sensing system, calibration diagram of phase angle signal (rad) vs. deflection (mm), has been experimentally determined by numerous deflection campaigns of CFRP honeycomb structure. Overall sensitivity of all fiber-optic sensors of about  $0,1 \text{ rad}/\mu\epsilon$  was determined out of phase angle signal (rad) vs. strain ( $\mu\epsilon$ ) calibration diagrams. It was also achieved very good linearity of all sensors in the entire deflection range from zero to 20mm. In respect of the initial requirements of resolution of  $0.1^\circ$  and deflection range of  $\pm 5^\circ$ , required resolution of phase angle signal should be of about 3rad that corresponds with about  $30\mu\epsilon$  of measured strain. It was proved that FOS3D system can fulfil these requirements since minimum detectable phase angle signal is of about 120mrad. Finally, the main goal of the project was successfully proved by experimentally verification of capability of the FOS3D system for simultaneous deflection measurement and damage detection with POD of more than 98% and localization accuracy of about 15mm.

## ACKNOWLEDGMENT

The research leading to these results has received funding from the European Union's Seventh Framework Programme (FP7/2007-2013) for the Clean Sky Joint Technology Initiative under grant agreement n\_CSJU-GAM-SFWA-2008-001.

## REFERENCES

- [1] P. M. M. Costa Aleixo. Morphing Aircraft Structures; Design and Testing an Experimental UAV, Instituto Superior Technico, Universidade Tecnica de Lisboa, Lisboa, 2007
- [2] B. O'Grady. Multi-Objective Optimization of a Three Cell Morphing Wing Substructure, PhD, University of Dayton, Dayton, 2010
- [3] W. Raither, M. Heymanns, A. Bergamini, P. Ermanni. Morphing Wing Structures with Controllable Twist Based on Adaptive Bending-Twist Coupling. *Smart Mater. Struct.* 22: 1-15, 2013.
- [4] A. Bergamini, R. Christen, B. Mag, M. Motavalli. A Sandwich Beam with Electrostatically Tunable Bending Stiffness, *Smart Mater. Struct.*, 15: 678-86, 2006.
- [5] Z. Djinovic, M. Scheerer, M. Tomic, M. Stojkovic, M. Schüller. Design and characterization of fiber-optic interferometric sensor for deflection and damage detection of morphing wing structures, Proceedings of the 9th International Workshop on Structural Health Monitoring, Stanford University, Stanford, CA, September 10-12, 2013.
- [6] C. K. Kirkendall, A. Dandridge. Overview of High-Performance Fiber-Optic Sensing, *J. Phys. D: Appl. Phys.*, 37: 197-216, 2004.
- [7] M. Scheerer, Z. Djinovic, M. Schüller. Fiber Optic System for Deflection and Damage Detection in Morphing Wing Structures, SPIE Conference on Smart Structure and Materials-Nondestructive Evaluation and Health Monitoring, San Diego, USA, 9th-14th March 2013.
- [8] M. Tomic, J. Elazar, Z. Djinovic. Low-coherence Interferometric Method for Measurement of Displacement Based on a 3x3 Fiber-Optic Directional Coupler, *J. Opt. A: Pure Appl. Opt.* 4:381-386, 2002.